Molecular Therapy
Nucleic Acids
Original Article

SMAD4-induced knockdown of the antisense long noncoding RNA BRE-AS contributes to granulosa cell apoptosis

Wang Yao,[1] Xing Du,[1] Jinbi Zhang,[1] Yang Wang,[1] Miaomiao Wang,[1] Zengxiang Pan,[1] and Qifa Li[1]

[1]College of Animal Science and Technology, Nanjing Agricultural University, Nanjing 210095, China

Antisense long noncoding RNAs (AS-lncRNAs), a sub-class of lncRNAs, are transcribed in the opposite direction from their overlapping protein-coding genes and are implicated in various physiological and pathological processes. However, their role in female reproduction remains largely unknown. Here, we report that *BRE-AS*, an AS-lncRNA transcript from intron 10 of the protein-coding gene *BRE*, is involved in granulosa cell (GC) apoptosis. Based on our previous RNA sequencing data, we identified 28 AS-lncRNAs as important in the initiation of porcine follicular atresia, with *BRE-AS* showing the most significant upregulation in early atretic follicles. In this study, gain- and loss-of-function assays demonstrated that *BRE-AS* induces early apoptosis in GCs. Mechanistically, *BRE-AS* acts in *cis* to suppress the expression of BRE, an anti-apoptotic factor, via direct interaction with the pre-mRNA transcript of the latter, inducing increased GC apoptosis. Notably, we also found that *BRE-AS* was upregulated in SMAD4-silenced GCs. SMAD4 was identified as a transcriptional repressor of BRE-AS because it inhibits *BRE-AS* expression and *BRE-AS*-mediated GC apoptosis. In conclusion, we not only identified a novel AS-lncRNA related to the early apoptosis of GCs and initiation of follicular atresia but also described a novel regulatory pathway, SMAD4/BRE-AS/BRE, coordinating GC function and female fertility.

INTRODUCTION

Long noncoding RNAs (lncRNAs) are defined as RNA transcripts of more than 200 nucleotides with no protein-coding potential, which function in multiple cellular processes, including cellular proliferation, development, differentiation, apoptosis, and autophagy.[1–4] lncRNAs are classified as intronic, intergenic, sense, bidirectional, and antisense on the basis of their genomic location and relationship with the protein-coding genes on the chromosome.[5] Antisense lncRNAs (AS-lncRNAs) are transcribed from the antisense strand of well-defined transcriptional units, mainly protein-coding genes.[6,7] Owing to their double-stranded RNA (dsRNA) formation, AS-lncRNAs are well known for regulating the sense transcript of protein-coding genes facilitated by multiple mechanisms, including interfering with splicing and translation,[8–10] affecting RNA stability,[11,12] and inducing RNA editing.[13]

Emerging evidence suggests that AS-lncRNAs are involved in various biological processes, such as X chromosome inactivation,[14,15] muscle atrophy,[9] stem cell pluripotency,[16] neural signal transduction,[17] immune response,[8] circadian clock function,[18] and even tumorigenesis.[18–20] Recently, a few reports have demonstrated that AS-lncRNAs are involved in female reproduction.[21,22] For example, lnc-Amhr2, an AS-lncRNA transcript from the 5′ regulatory region of the *Amhr2* gene, which is essential for various reproductive functions, has been shown to induce *Amhr2* transcription in mouse granulosa cells (GCs) by enhancing the *Amhr2* promoter activity.[21] In human cumulus cells, HAS2-AS1 inhibition results in decreased GC migration and HAS2 expression, a marker of the cumulus expansion and ovulation.[22] In addition, dysregulation of several AS-lncRNAs (e.g., *CHL1-AS1*, *CHL1-AS2*, and human zinc finger antisense 1 [*ZFAS1*]) causes ovarian dysfunction and diseases such as ovarian endometriosis or polycystic ovary syndrome.[23,24]

Mammalian folliculogenesis is an intricate process that begins with the establishment of a primordial follicle pool in fetal life,[25] with only two final outcomes: either mature and ovulation or atresia and degeneration.[26,27] The latter is the ultimate fate of most follicles. Follicular atresia has been shown to be triggered by GC apoptosis[28,29] and is also affected by oocyte apoptosis.[30] Increasing evidence demonstrates that both follicular atresia and GC apoptosis are regulated by numerous factors, such as gonadotropins (e.g., follicle-stimulating hormone [FSH]),[31] steroid hormones (e.g., estrogen),[32] cytokines (e.g., transforming growth factor beta 1 [TGF-β1]),[33] and noncoding RNAs, including microRNAs (miRNAs), lncRNAs, and circular RNAs (circRNAs).[3,34,35] However, the role of AS-lncRNAs in follicular atresia and GC apoptosis remains largely unknown. In this study, we aimed to identify AS-lncRNAs related to the initiation of follicular atresia. Furthermore, we investigated the mechanism underlying the initiation of follicular atresia induced by *BRE-AS*, the most significantly upregulated AS-lncRNA in early atretic follicles, and sought to understand the

Received 24 November 2020; accepted 7 May 2021;
https://doi.org/10.1016/j.omtn.2021.05.006.

Correspondence: Qifa Li, College of Animal Science and Technology, Nanjing Agricultural University, Nanjing 210095, China.
E-mail: liqifa@njau.edu.cn

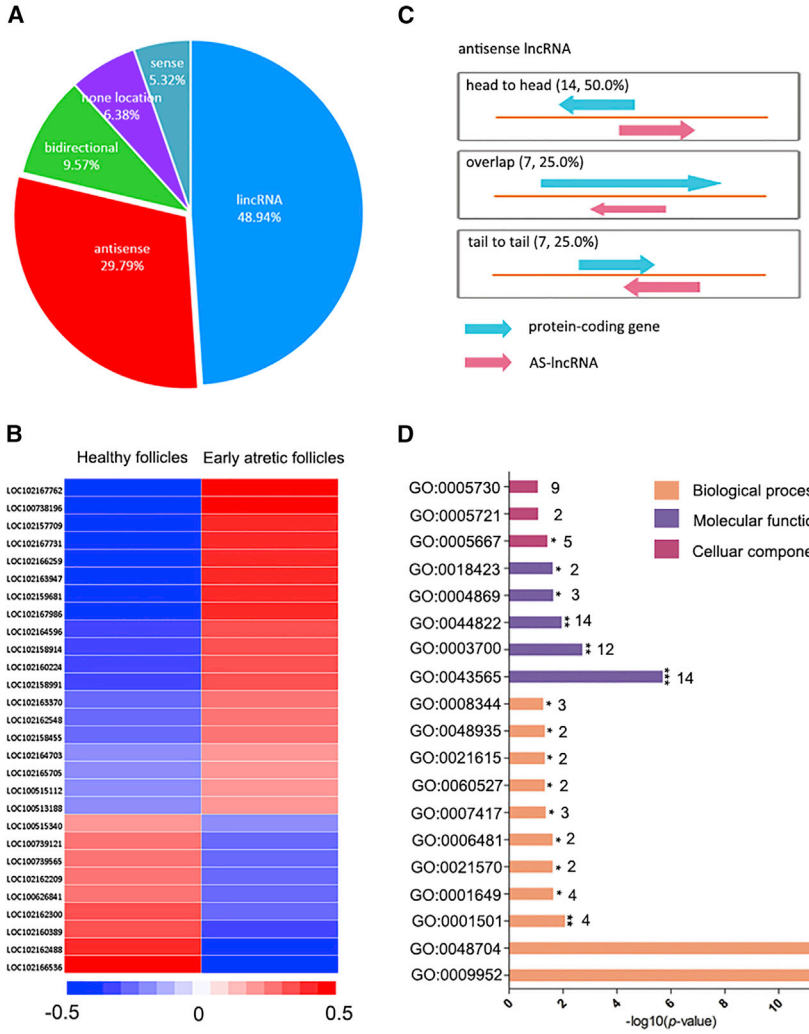

Figure 1. Identification of AS-lncRNAs related to initiation of follicular atresia

(A) Pie chart showing classification of DELs in follicles from healthy and early atretic samples. (B) Heatmap showing the DEAS-lncRNAs in early atretic follicles compared with that in healthy follicles. (C) Schematic showing sub-classification of DEAS-lncRNAs. (D) GO functional enrichment of the *cis*-target mRNAs for DEAS-lncRNAs. The *cis*-target mRNAs were selected within the range of 200 kb in the upstream and downstream of DEAS-lncRNAs. GO analysis was performed using an online tool, DAVID (https://david.ncifcrf.gov/). The number of enrichment genes in each GO term was annotated at the end of the bar. Each group is represented by mean ± SEM; *p < 0.05. **p < 0.01. ***p < 0.001.

mechanism underlying high *BRE-AS* expression in early atretic follicles.

RESULTS

Differentially expressed AS-lncRNAs during porcine follicular atresia

We previously identified 94 differentially expressed lncRNAs (DELs) in follicles from healthy and early atretic samples using RNA sequencing (RNA-seq) (unpublished). Based on genomic location, we classified these DELs into long intergenic noncoding RNAs (lincRNAs) (46, 48.94%), bidirectional (9, 9.57%), sense (5, 5.32%), AS-lncRNAs (28, 29.79%), and lncRNAs that cannot be located within the genome (6, 6.38%) (Figure 1A). This shows that other than lincRNAs, AS-lncRNAs are the most abundant DELs in ovarian follicles during follicular atresia. In total, 28 differentially expressed AS-lncRNAs (DEAS-lncRNAs) (Figure 1B) were then sub-classified into three classical models: head-to-head (14, 50.0%), tail-to-tail (7, 25.0%), and overlap (7, 25.0%) (Figure 1C; Table S1). To further understand the potential function of these DEAS-lncRNAs, we performed a Gene Ontology (GO) enrichment analysis on the *cis*-target mRNAs of these DEAS-lncRNAs. Seventeen significant GO terms belonging to three GO categories, namely, biological process (BP) (11), cell component (CC) (5), and molecular function (MF) (1), were identified (Figure 1D; Table S2). GO terms in the BP category mainly included the anterior/posterior pattern specification (GO: 0009952), embryonic skeletal system morphogenesis (GO: 0048704), and skeletal system development (GO: 0001501). Those in the MF category mainly included sequence-specific DNA binding (GO: 0043565), transcription factor activity (GO: 0003700), and poly(A) RNA binding (GO: 0044822). The GO term in the CC category was transcription factor complexes alone (GO: 0005667). These data suggest that these DEAS-lncRNAs are related to the initiation of follicular atresia, possibly through the regulation of several important GO pathways.

BRE-AS is related to porcine follicular atresia

LOC102157709 is the most upregulated DEAS-lncRNA in early atretic follicles compared with that in healthy follicles (Figure 2A), indicating that it is strongly related to the initiation of follicular atresia. Therefore, *LOC102157709* was further investigated. Rapid amplification of cDNA ends (RACE) assay showed that the full length of porcine *LOC102157709* RNA was 468 bp (GenBank: MZ090592) (Figures 2B and 2C). Genomic location analysis showed that *LOC102157709* is embedded within intron 10 of the porcine brain- and reproductive-organ-expressed protein (*BRE*) gene, and transcribed from the antisense sequence of this gene (Figure 2D), allowing us to refer to this as *BRE-AS*. The *BRE-AS* gene consists of two exons and one intron (Figure 2D), and the online tool coding potential assessment tool (CPAT) further

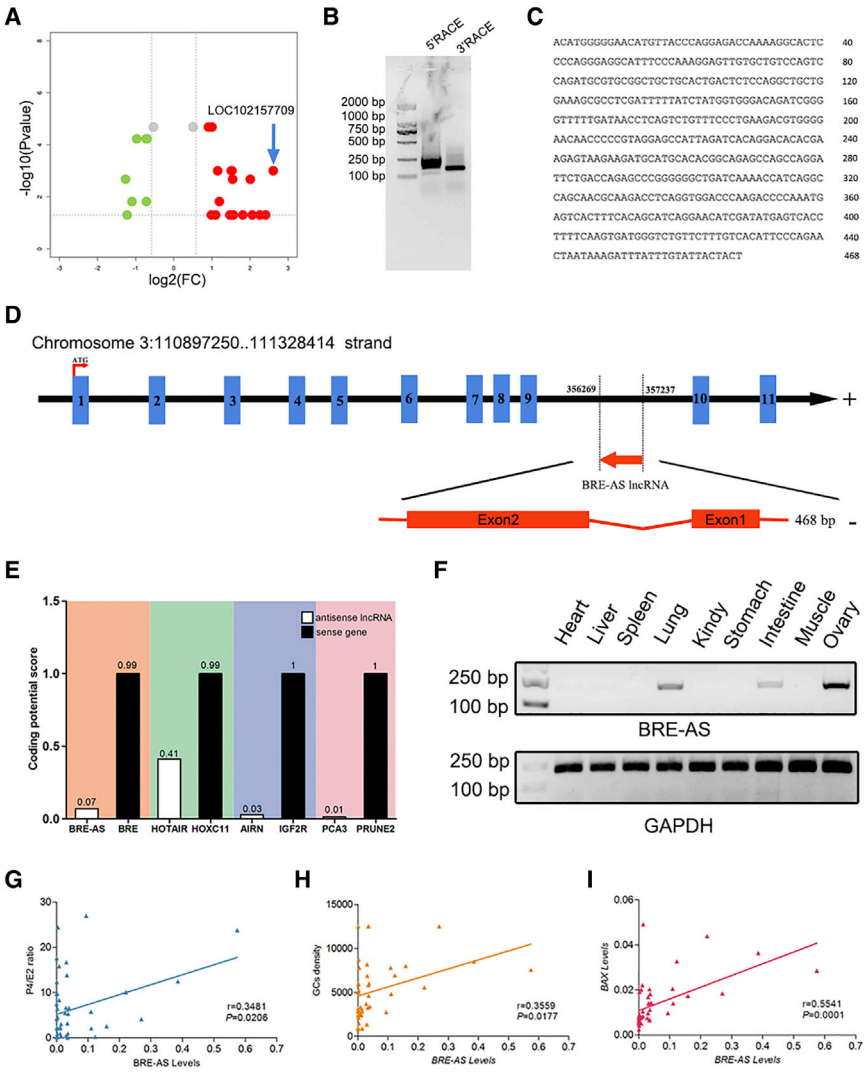

Figure 2. Identification and characterization of BRE-AS in pigs

(A) DEAS-lncRNAs are shown in the Ma plot. The horizontal axis represents logarithm of fold change to the base 2, and the vertical shows the negative logarithm of p value to the base 10. (B) RACE assay. The full length of *LOC102157709* was obtained by RACE assay using a SMARTer RACE cDNA Amplification Kit, and amplified products of 5′ and 3′ end are shown in agarose gel. (C) The full-length RNA sequence of the porcine *LOC102157709* gene. (D) Schematic showing genomic location of *LOC102157709*. *LOC102157709* is embedded within intron 10 of the porcine *BRE* gene and transcribed from the antisense sequence of this gene, so named *BRE-AS*. (E) The potential coding ability of *BRE-AS* and *BRE* were predicted by Coding Potential Assessment Tool (CPAT) tool. *HATAIR*, *ARIN*, and *PCA3* are known AS-lncRNAs, and *HOXC11*, *IGF2R*, and *PRUNE2* are their counterpart sense genes, respectively. (F) The expression pattern of *BRE-AS* in nine different tissues of pigs. *GAPDH* was used for internal control. (G–I) The correlation analysis between follicular *BRE-AS* levels and the P4/E2 ratio (G) and GC density (H), in follicular fluid, *BAX* mRNA levels (I) in follicles (n = 44). Each group were represented by mean ± SEM.

confirmed that *BRE-AS* is an AS-lncRNA with no protein-coding potential (Figure 2E). *BRE-AS* tissue expression patterns showed that it is specifically highly expressed in the ovary, lung, and intestine (Figure 2F). To further confirm the relationship between *BRE-AS* and follicular atresia *in vivo*, correlation analysis between follicular *BRE-AS* levels and the ratio of progesterone and 17β-estradiol concentration (P4/E2) and GC density, both biomarkers of follicular atresia in follicular fluid, was performed. The results showed that follicular *BRE-AS* levels were positively correlated with the P4/E2 ratio and GC density in follicular fluid (Figures 2G and 2H), indicating that *BRE-AS* is related to follicular atresia *in vivo*. Follicular atresia is well known to be triggered by GC apoptosis.[28] We also showed that follicular *BRE-AS* levels were significantly associated with mRNA abundance of multiple pro-apoptotic genes, such as *BAX*, *Caspase-3*, and *Caspase-8* (Figure 2I; Figure S1). These data suggest that *BRE-AS* is related to ovarian functions, especially follicular atresia.

BRE-AS induces early apoptosis of GCs

To investigate the role of *BRE-AS* in ovarian functions, especially follicular atresia, we overexpressed and knocked down *BRE-AS* in porcine GCs by transfection with a vector pcDNA3.1-BRE-AS or BRE-AS-specific small interfering RNA (BRE-AS-siRNA) (Figures 3A and 3B). Flow cytometry showed that *BRE-AS* overexpression strongly increased the GC apoptosis rate, especially the early apoptosis rate (Figure 3C). Furthermore, mRNA transcript ratios for anti-apoptotic *BCL2* and pro-apoptotic *BAX* (*BCL2*/*BAX*) were decreased in *BRE-AS*-overexpressing GCs (Figure 3D). Conversely, *BRE-AS* knockdown decreased the GC apoptosis rate, especially the early apoptosis rate (Figure 3E), and increased the *BCL2*/*BAX* ratio in GCs (Figure 3F). These results suggest that *BRE-AS* induces the early apoptosis of GCs, thereby initiating follicular atresia.

BRE-AS modulates BRE expression by binding to its pre-mRNA

AS-lncRNAs play a critical biological role via their regulation of and interaction with their counterpart sense genes.[36] Therefore, we assessed whether *BRE-AS* affects BRE expression in GCs. As expected, BRE mRNA and protein levels were decreased in *BRE-AS*-overexpressing GCs (Figures 4A and 4B). In contrast, these levels were increased in *BRE-AS*-silenced GCs (Figures 4C and 4D), suggesting that *BRE-AS* is a negative modulator of BRE in GCs. To further elucidate the underlying mechanism by which *BRE-AS* inhibits BRE, we first investigated the subcellular distribution of *BRE-AS* in GCs. As shown in Figure 4E, *BRE-AS* was expressed in both the nucleus and

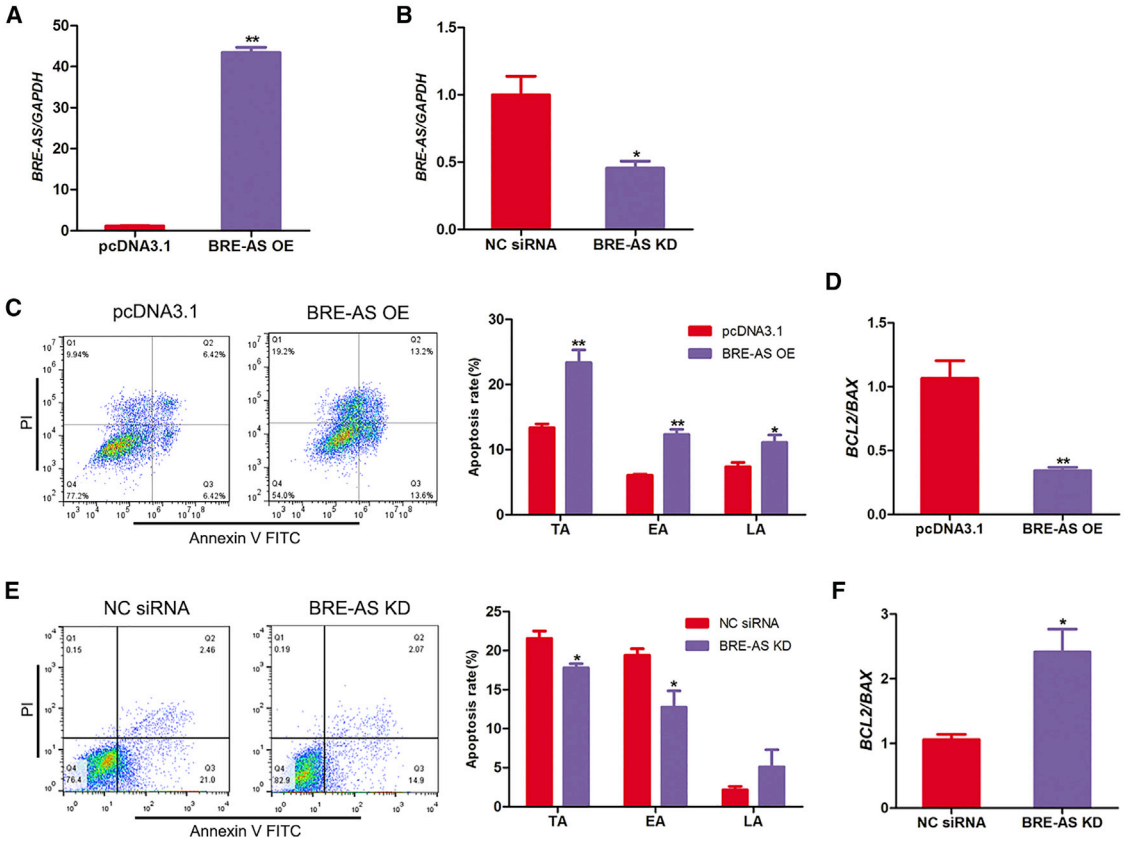

Figure 3. BRE-AS induces GC apoptosis

(A and B) The efficiency of overexpression (A) or silencing (B) of *BRE-AS* in GCs by transfecting pcDNA3.1-BRE-AS vector or BRE-AS-siRNA were verified using qRT-PCR. (C and D) Overexpression of *BRE-AS* promotes cell apoptosis. GCs were treated with pcDNA3.1-BRE-AS, apoptosis rate was detected by fluorescence-activated cell sorting (FACS) (C), *BCL2* and *BAX* levels were determined by qRT-PCR, and *BCL2*/*BAX* ratio was calculated (D). TA, total apoptosis rate. EA, early apoptosis rate. LA, later apoptosis rate. (E and F) Silencing of *BRE-AS* inhibits cell apoptosis. GCs were treated with BRE-AS-siRNA, apoptosis rate was determined by FACS (E), *BCL2* and *BAX* levels were detected by qRT-PCR, and *BCL2*/*BAX* ratio was calculated (F). Each group is represented by mean ± SEM; *$p < 0.05$, **$p < 0.01$.

cytoplasm, and co-RNA-fluorescence *in situ* hybridization (co-RNA-FISH) showed that BRE-AS and *BRE* pre-mRNA hybridized within the same nuclear foci (Figure 4F). Furthermore, when RNAs isolated from GCs were treated with RNase I, an RNase that specifically degrades single-stranded RNA (ssRNA), the overlapping region in both transcripts was found to be protected from degradation, indicating that *BRE-AS* and *BRE* pre-mRNA form dsRNA in the nuclei of GCs (Figure 4G). In addition, *BRE-AS* suppressed the pre-mRNA expression of *BRE* in GCs (Figure 4H). These data suggest that *BRE-AS* binds to *BRE* pre-mRNA to control *BRE* expression in GCs.

BRE-AS induces GC apoptosis via downregulation of BRE expression

To assess the role of *BRE* in GC apoptosis, we overexpressed or silenced *BRE* in GCs by transfecting with pcDNA3.1-BRE or BRE-siRNA, respectively (Figure S2). BRE overexpression decreased the apoptosis rate of GCs (Figure 5A) and increased the *BCL2*/*BAX* ratio (Figure 5B), whereas BRE inhibition had the opposite effect (Figures 5C and 5D), indicating that BRE attenuates GC apoptosis, which is contrary to the effect of *BRE-AS*. Additionally, BRE overexpression relieved the GC apoptosis induced by *BRE-AS* (Figure 5E), whereas *BRE* silencing inhibited the reduction in apoptosis caused by *BRE-AS* knockdown in GCs (Figure 5F). Taken together, these results suggest that *BRE-AS* induces GC apoptosis via the downregulation of BRE expression.

SMAD4 is an inhibitor of BRE-AS in GCs

Notably, our previous RNA-seq data showed that *BRE-AS* is also a DEL in SMAD4-silenced GCs (Figure 6A).[37] Quantitative reverse transcription-polymerase chain reaction (qRT-PCR) revealed that *BRE-AS* is upregulated in SMAD4-silenced GCs (Figure 6B), which is consistent with our RNA-seq data. Furthermore, the overexpression of SMAD4 by transfection with pcDNA3.1-SMAD4 reduced *BRE-AS* expression in GCs (Figure 6C). In addition, the silencing of SMAD4 increased BRE expression (Figures 6D and 6E), whereas the overexpression of

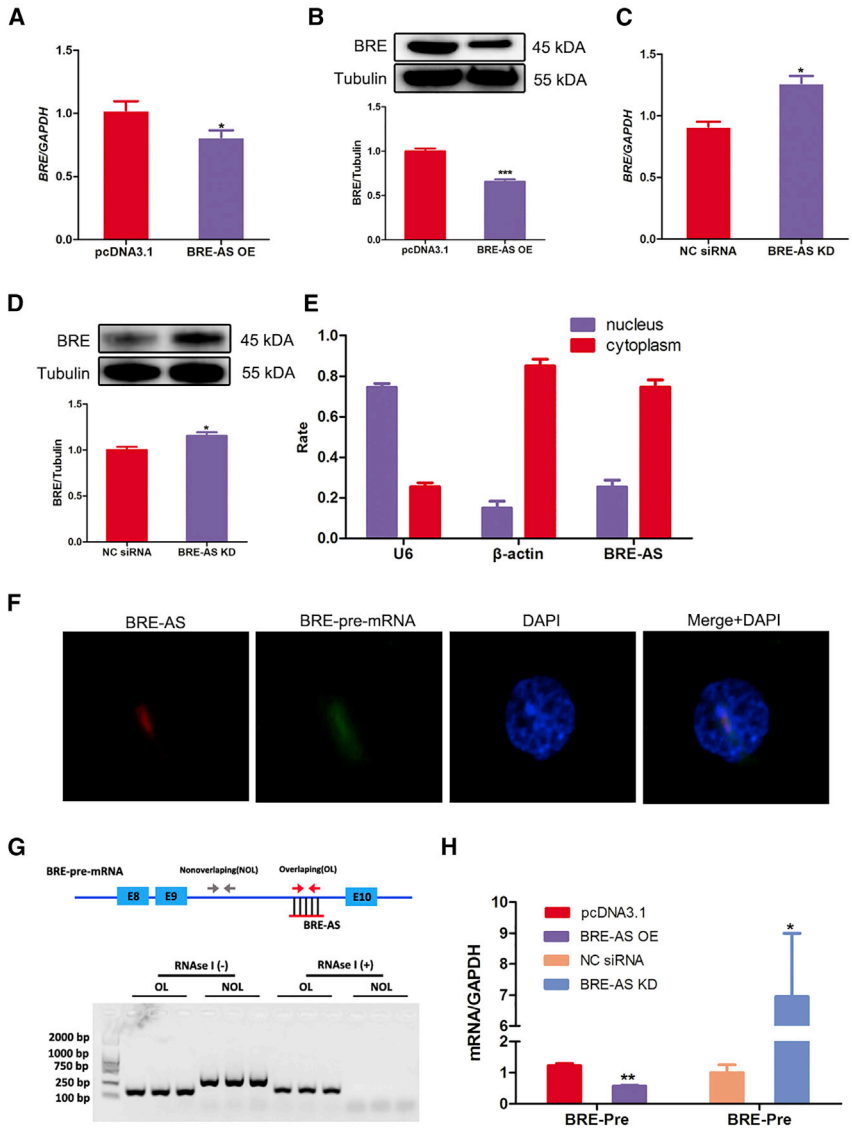

Figure 4. BRE-AS suppresses BRE expression through forming an RNA-RNA double-strand

(A and B) mRNA (A) and protein (B) levels of BRE in BRE-AS-overexpressing GCs were measured by qRT-PCR and western blot. (C and D) mRNA (C) and protein (D) levels of BRE in BRE-AS-silencing GCs. (E) The subcellular localization of *BRE-AS* in GCs. Levels of *BRE-AS*, cytoplasmic β-actin, and nuclear U6 in cytoplasm and nuclear isolated form GCs were determined by qRT-PCR. (F) Co-location assay of *BRE-AS* and *BRE* pre-mRNA were performed by RNA-FISH. Nucleus was stained with DAPI (blue), *BRE-AS* was dyed with BRE-AS-specific probe (red), and *BRE* pre-mRNA was dyed with *BRE* pre-mRNA-specific probe (green). (G) Ribonuclease protection assay (RPA) was performed using non-overlapping and overlapping primer, and qRT-PCR showed the overlapping part of both transcripts was protected from degradation induced by RNaseI treatment. (H) *BRE-AS* controls *BRE* pre-mRNA levels in GCs. *BRE* pre-mRNA levels were detected by qRT-PCR in BRE-AS-overexpressing or -silencing GCs. Each group is represented by mean ± SEM; $^{*}p < 0.05$, $^{**}p < 0.01$.

SMAD4 had the opposite effect in targeted cells (Figures 6F and 6G). However, this regulatory effect of SMAD4 on BRE expression was reversed by BRE-AS (Figures 6H and 6I), indicating that SMAD4 regulates the downstream target of *BRE-AS* via *BRE-AS* in GCs. These data suggest that SMAD4 is an inhibitor of *BRE-AS* in GCs.

SMAD4 is a transcriptional repressor of BRE-AS in GCs

SMAD4 is a well-known transcription factor.[3,38] To elucidate the molecular mechanism by which SMAD4 inhibits *BRE-AS* in GCs, we first isolated a 1,100-bp sequence from the *BRE-AS* promoter region. Three SMAD4-binding elements (SBEs) were observed in this region (Figure 7A; Figure S3), and a DNA sequence from −161 nt to +148 nt of the promoter was identified as a putative core promoter region of *BRE-AS* in GCs using deletion constructs (Figure 7B). Furthermore, the activity of the *BRE-AS* core promoter was significantly decreased by SMAD4 overexpression (Figure 7C), whereas it was dramatically increased by SMAD4 knockdown (Figure 7D), revealing that SMAD4 can regulate the promoter activity of *BRE-AS*. Chromatin immunoprecipitation (ChIP) assay showed that SMAD4 directly binds to the SBE site in the core promoter of *BRE-AS* but not outside the promoter region (Figure 7E). Overall, these results and our previous data showed that SMAD4 is a transcriptional repressor of *BRE-AS* in GCs.

BRE-AS mediates SMAD4-induced inhibition of GC apoptosis

SMAD4 serves as an anti-apoptotic factor in porcine GCs.[38] To determine whether SMAD4 controls GC apoptosis via *BRE-AS*, GCs were co-transfected with pcDNA3.1-SMAD4 and pcDNA3.1-BRE-AS or SMAD4-siRNA and BRE-AS-siRNA. As expected, the overexpression of SMAD4 reduced the GC apoptosis rate; however, this anti-apoptotic effect was reversed by *BRE-AS* overexpression (Figure 8A). In contrast, GC apoptosis was induced by SMAD4 knockdown; however, this was blocked by BRE-AS-siRNA (Figure 8B). Collectively, these results suggest that *BRE-AS* is a functional target of SMAD4 and mediates SMAD4-induced inhibition of GC apoptosis.

DISCUSSION

Atresia is the ultimate fate of most ovarian follicles and limits the utilization efficiency of follicles and fertility potential in females. Follicular atresia is affected by many factors, such as follicular fluid factors,[31,39,40] cell-death-related factors,[26,29,41,42] and epigenetic mediators including miRNAs, lncRNAs, and circular RNAs.[3,32,43] Here, we found that

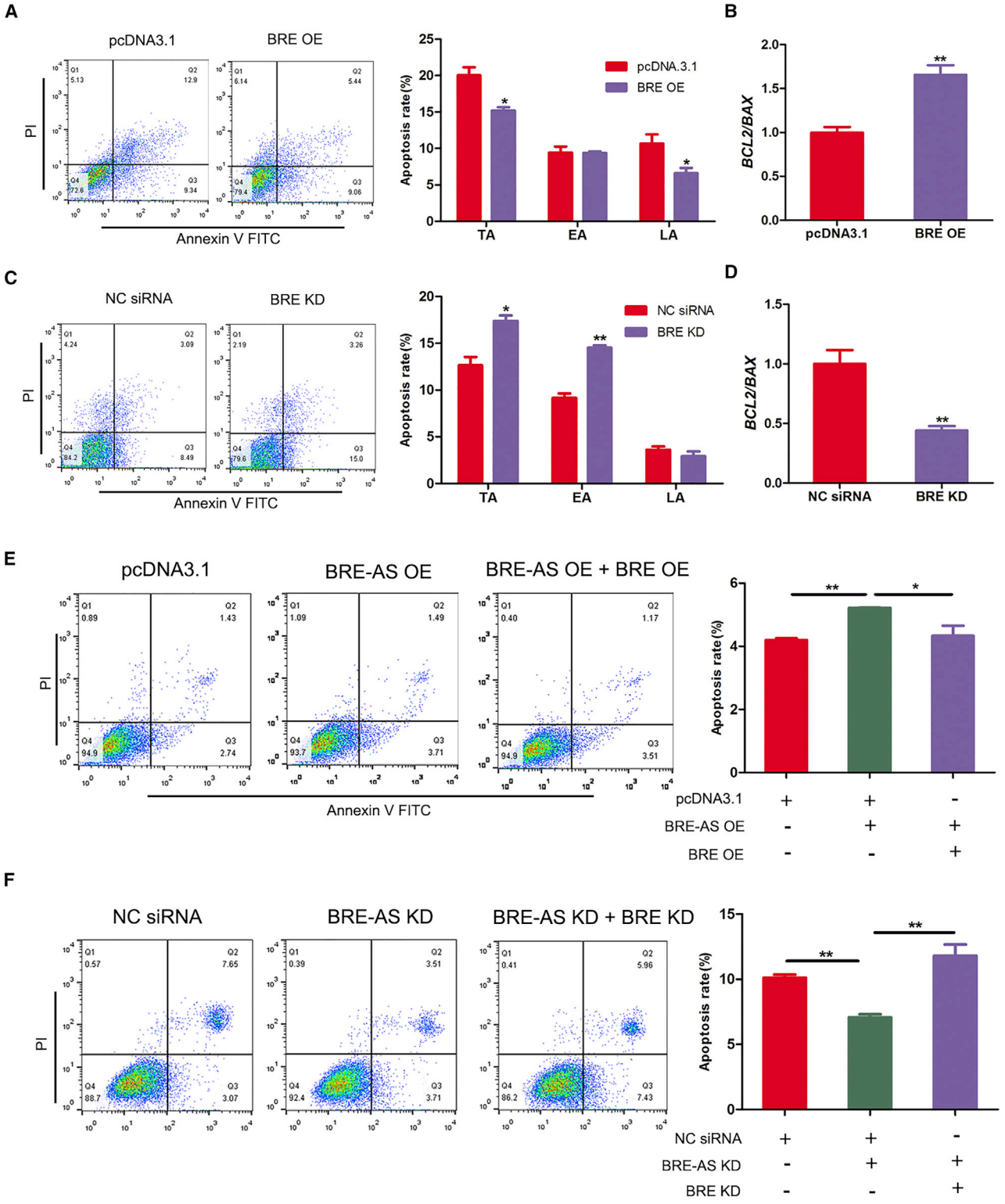

(legend on next page)

AS-lncRNAs are related to the initiation of porcine follicular atresia and demonstrated that *BRE-AS* induces GC apoptosis, the primary cause of follicular atresia, by suppressing the protein-coding gene *BRE*, which encodes an anti-apoptotic factor. In addition, we showed that the anti-apoptotic factor SMAD4 is a transcriptional repressor of *BRE-AS* in GCs.

This study demonstrated for the first time that AS-lncRNAs participate in the regulation of follicular atresia and that *BRE-AS*, the most upregulated AS-lncRNA during follicular atresia, regulates the early apoptosis of GCs. Follicular atresia is triggered by GC apoptosis. Therefore, follicular-atresia-related factors including lncRNAs are usually involved in GC apoptosis.[3,44] Noncoding RNA involved in the follicular atresia (*NORFA*), a lincRNA, was the first functional lncRNA linked to increased fecundity in Erhualian pigs, one of the most prolific pig breeds known worldwide, and is involved in follicular development and atresia via the inhibition of GC apoptosis.[3] SMAD4-dependent noncoding RNA (*SDNOR*), an lncRNA, forms a regulatory axis with miR-29c to mediate crosstalk between the TGF-β and Wnt signaling pathways, inhibiting GC apoptosis and follicular atresia.[44] Although there are no other reports describing the relationship between AS-lncRNAs and follicular atresia, the relationship between *ZFAS1*, an AS-lncRNA, and the regulation of GC apoptosis has recently been reported.[21]

BRE, also known as BABAM2 or BRCC45, is required for maintaining genomic integrity and plays a key role in DNA repair and anti-apoptotic responses.[45,46] BRE is highly expressed in reproductive systems and is strongly involved in follicular development and atresia.[29,47] A recent report showed that BRE mutants promote follicular atresia by inducing GC apoptosis via changes in the DNA damage repair pathways.[29] In this study, we showed that BRE mediates *BRE-AS*-enhanced GC apoptosis, demonstrating that BRE is also an anti-apoptotic factor in porcine GCs. Notably, BRE has been identified as an anti-apoptotic factor in multiple cell types, including mouse hepatocytes,[40] human hepatocellular carcinoma cells,[48] lung cancer cells,[49] and esophageal squamous cell carcinoma cells.[50] Taken together, our findings describe the underlying regulatory mechanism facilitating *BRE-AS*-induced apoptosis in porcine GCs and further verify that BRE is an anti-apoptotic factor in the ovarian GCs of mammals.

AS-lncRNAs are a type of natural antisense transcripts (NATs), which are strongly associated with their counterpart sense genes.[51–53] Increasing evidence suggests that AS-lncRNAs perform their biological functions primarily through the regulation of their counterpart sense genes by forming an RNA-RNA duplex or RNA-DNA triplex with their counterpart sense genes.[12,22,54,55] In this study, we showed that *BRE-AS* suppresses *BRE* expression in porcine GCs by forming an RNA-RNA duplex with its pre-mRNA transcript. This dsRNA model has been shown to be involved in RNA splicing, RNA editing, and RNA silencing.[10,21,56] For example, *SAF*, an antisense lncRNA of the apoptotic gene *Fas*, interacts with the pre-mRNA of the *Fas* receptor and recruits splicing factor 45 (*SPF45*) to facilitate the deletion of exon 6. This variant of FasΔEx6 produces soluble sFas protein and blocks FasL-induced apoptosis.[56] The dsRNA structure can also trigger RNA editing of the pre-mRNA sequence of the sense transcript.[21] Prostate cancer antigen 3 (*PCA3*), an antisense intronic lncRNA of *PRUNE2*, binds to intron 6 of *PRUNE2* pre-mRNA and induces adenosine-to-inosine RNA editing mediated by ADAR2, which facilitates endogenous PRUNE2 silencing and tumorigenesis.[21] In addition, the nuclear-enriched antisense transcript *GLS-AS* is involved in pancreatic cancer metabolism and is known to suppress GLS expression at the post-transcriptional level via the production of a dsRNA construct including the AS-lncRNA sequence and the *GLS* pre-mRNA transcript. This dsRNA structure triggers ADAR/Dicer-dependent RNA interference.[57]

SMAD4 is the only Co-SMAD protein in the TGF-β signaling pathway and plays an important role in GC function by acting as an anti-apoptotic protein.[36,37] Many anti-apoptotic mechanisms of SMAD4 in GCs have been investigated, and the regulation of noncoding RNAs (e.g., miRNAs and lncRNAs) is one of the important mechanisms.[44,58] SMAD4 controls GC apoptosis directly via miRNAs through two mechanisms: (1) influencing miRNA biosynthesis,[58] and (2) regulating single miRNA expression as a transcription factor.[59,60] However, little is known about the interactions between SMAD4 and lncRNAs in the regulation of GC apoptosis. In this study, we showed that SMAD4 functions as a transcription factor to inhibit GC apoptosis by direct binding with the *BRE-AS* promoter region. Du et al.[3] demonstrated that SMAD4 binds to the SBE motif in the promoter region of lncRNA *SDNOR* to promote *SDNOR* expression and control *SDNOR*-mediated apoptosis in porcine GCs. In addition, SMAD4 has been shown to be a transcriptional regulator of several lncRNAs in other cell types, such as lncRNA *PCAT7* in prostate cancer cells,[61] lncRNA 9884 in renal inflammation cells,[62] *LINP1* in lung cancer cells,[63] and *LIN-LET* in bladder cancer cells.[64] Our findings provide new evidence for SMAD4 regulation of GC apoptosis by lncRNAs, especially AS-lncRNAs.

Our study is the first to identify the relationship between AS-lncRNAs and the initiation of follicular atresia. We demonstrated that *BRE-AS* initiates follicular atresia by inducing early apoptosis in GCs. Furthermore, *BRE-AS* suppresses host BRE expression by forming an

Figure 5. BRE mediates BRE-AS induction of GC apoptosis

(A and B) GCs were transfected with pcDNA3.1-BRE, apoptosis rate was determined by FACS (A), *BCL2* and *BAX* levels were detected by qRT-PCR, and *BCL2*/*BAX* ratio was calculated (B). (C and D) GCs were transfected with BRE-siRNA, apoptosis rate was determined by FACS (C), *BCL2* and *BAX* levels were detected by qRT-PCR, and *BCL2*/*BAX* ratio was calculated (D). (E) GCs were co-transfected with pcDNA3.1-BRE-AS and pcDNA3.1-BRE, and apoptosis rate was determined by FACS. (F) GCs were co-transfected with BRE-AS-siRNA and BRE-siRNA, and apoptosis rate was determined by FACS. Each group has at least 3 replicates. Each group is represented by mean ± SEM; *$p < 0.05$, **$p < 0.01$.

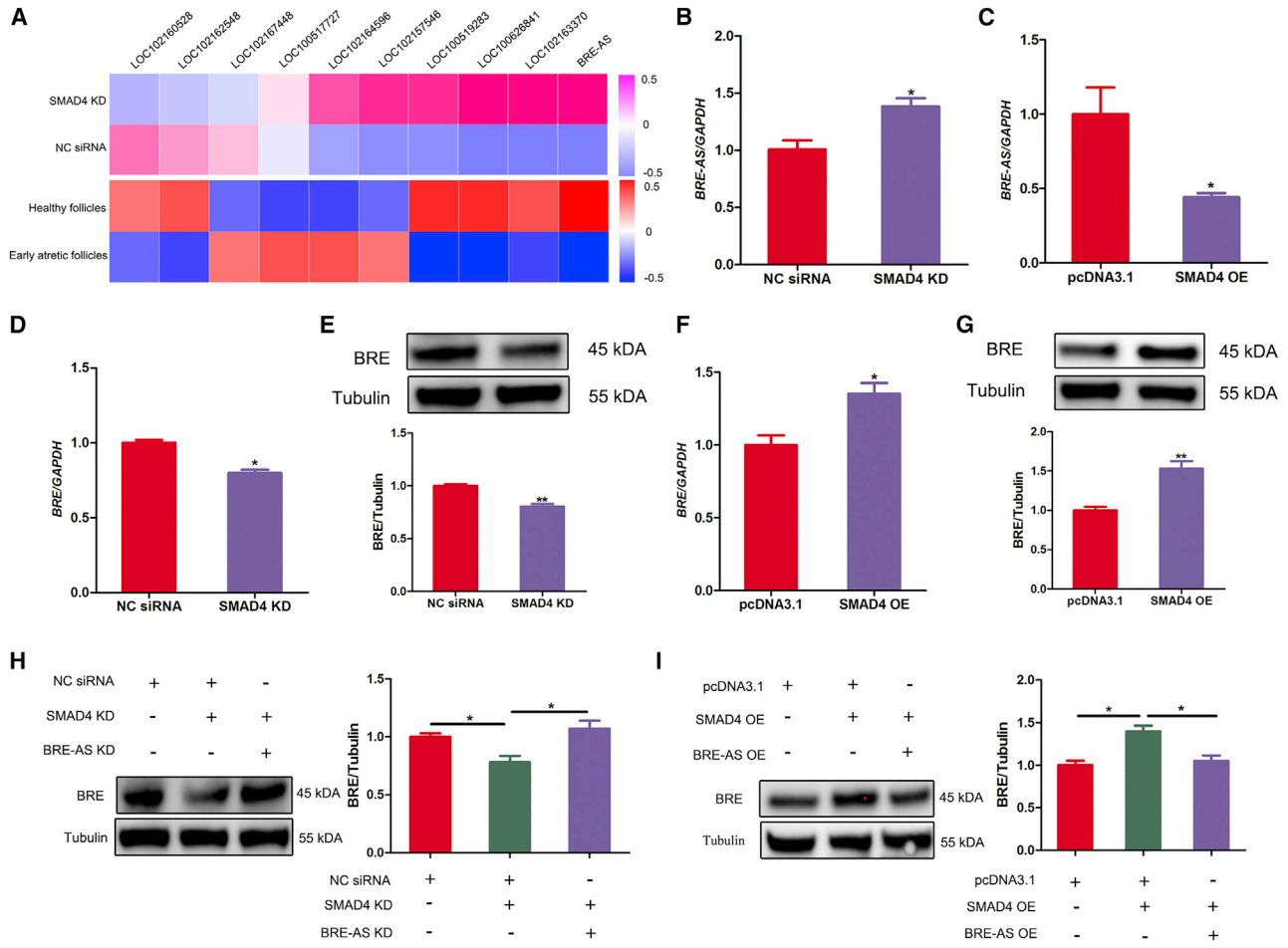

Figure 6. SMAD4 controls expression of BRE-AS and BRE axis in GCs

(A) Heatmap showing DELs in both healthy follicles versus early atretic follicles, and control versus SMAD4-silencing porcine GCs. RNA-seq data of SMAD4-silenced porcine GCs were obtained from our previous study.[26] (B and C) *BRE-AS* levels in SMAD4-silencing (B) or -overexpressing (C) GCs were measured by qRT-PCR. (D and E) BRE mRNA (D) and protein (E) levels in SMAD4-silencing GCs were detected by qRT-PCR and western blot. (F and G) BRE mRNA (F) and protein (G) levels in SMAD4-overexpressing GCs were detected by qRT-PCR and western blot. (H and I) BRE-AS-siRNA and SMAD4-siRNA (H), or pcDNA3.1-BRE-AS and pcDNA3.1-SMAD4 (I) were co-transfected into GCs, and BRE protein levels were detected by western blot. Each group has at least 3 replicates. Each group is represented by mean ± SEM; *p < 0.05, **p < 0.01.

RNA-RNA duplex with the *BRE* pre-mRNA transcript and facilitates GC apoptosis. In addition, we identified SMAD4 as a transcriptional repressor of *BRE-AS* and described a novel pathway for the regulation of follicular atresia and GC apoptosis, that is, the SMAD4/*BRE-AS*/BRE pathway (Figure 8C). Overall, our findings provide new insights into the epigenetic mechanisms underlying follicular atresia and female fertility. AS-lncRNA *BRE-AS* is expected to become a new target and non-hormone drug for molecular therapy of follicular atresia and other ovarian diseases.

MATERIALS AND METHODS

lncRNA locus classification

Data on DELs in healthy and early atresia follicle samples from porcine ovaries were obtained from our previous RNA-seq study (unpublished), and the DELs were classified into locus biotypes according to their genomic distribution patterns.[64] lncRNAs were defined as either genic ($\leq$5 kb) or intergenic (>5 kb) using a 5 kb cutoff for nearby protein-coding genes. Genic lncRNAs were then further categorized as bidirectional, sense, or antisense based on their transcriptional orientation and start site with respect to any nearby protein-coding locus (Figure S4).

Bioinformatics analysis

Differential expression analysis of AS-lncRNAs was performed using the DESeq2 pack in R project (https://www.r-project.org/), and the *cis* roles of these DEAS-lncRNAs were determined using GO enrichment analysis, based on the coding genes up to 200 kb upstream or downstream of the DEAS-lncRNAs. This analysis was performed using the DAVID 6.8 database (https://david.ncifcrf.gov/tools.jsp), and a p value < 0.05 was considered to indicate statistical significance. The

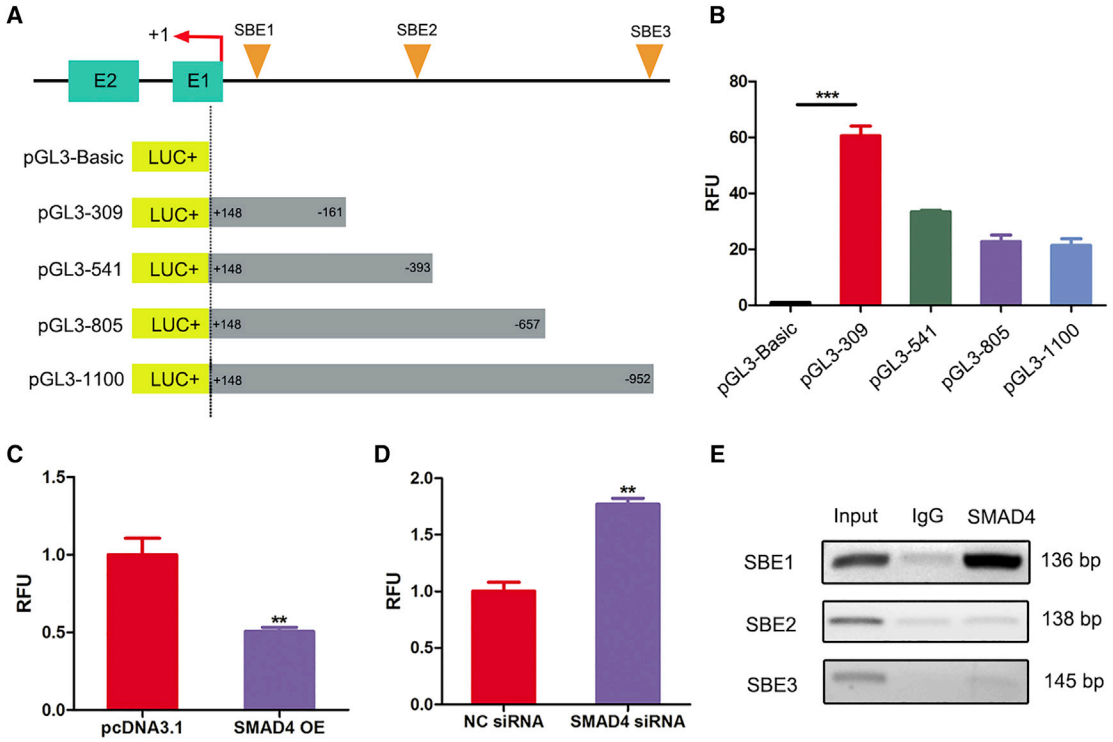

Figure 7. SMAD4 is a transcriptional repressor of BRE-AS

(A) Schematic showing the deletion constructs of *BRE-AS*. Four fragments (−161 nt/+148 nt, −393 nt/+148 nt, −657 nt /+148 nt, and −952 nt /+148 nt) were amplified from the promoter region of *BRE-AS* and inserted into the pGL3-basic reporter vector. The transcriptional start site was defined as +1. The triangles represent the putative SMAD-binding sites (SBEs). (B–D) Luciferase assay. Deletion constructs were transfected (B), or pGL3-309 and pcDNA3.1-SMAD4 (C), or pGL3-309 and SMAD4-siRNA (D) were co-transfected into GCs, and luciferase activity was detected. (E) ChIP assay. IgG was used as negative control. Each group has at least 3 replicates. Each group is represented by mean ± SEM; *$p < 0.05$, **$p < 0.01$.

locations of the AS-lncRNAs and their nearby genes were annotated using the National Center for Biotechnology Information database (https://www.ncbi.nlm.nih.gov/). The CPAT website tool[65] (http://lilab.research.bcm.edu/cpat/) was used to predict the protein-coding ability of AS-lncRNAs. The transcriptional factors in the promoter region of *BRE-AS* were identified using the JASPAR database (http://jaspar.genereg.net/).

Follicle collection and P4 or E2 detection

Follicles were collected as previously described.[35] Briefly, antral follicles, 3–5 mm in diameter, were dissociated from the ovaries by surgical tweezers and scalpels. After tearing the follicular membrane with forceps, the follicular fluid was isolated by centrifugation at 1,000 rpm for 1 min. All animal experiments were approved by the Ethical Committee of Nanjing Agricultural University. The GC density was counted using a hemocytometer in follicular fluid diluted in phosphate-buffered saline (PBS) (1:10) under a light microscope. For P4 or E2 detection, after centrifugation for 3 min at 1,000 rpm, the supernatant of follicular fluid was diluted at 1:100 in PBS, and radioimmunoassay was performed to measure steroid hormone levels by using iodine [125I] P4 or E2 RadioImmunoassay Kit (North Institute, Beijing, China) in Jinling Hospital (Nanjing, China) according to the manufacturer's instructions.

RNA isolation and qRT-PCR

Total RNA from porcine tissues, ovarian follicles (3–5 mm), or GCs were isolated using a High-Purity Total RNA Extraction Kit (Bioteke, Beijing, China), and cDNAs were reverse-transcribed using a HiScript Q RT SuperMix kit (Vazyme Biotech, Nanjing, China) according to the manufacturer's instructions. qRT-PCR was performed using an AceQ qPCR SYBR Green Master Mix (Vazyme Biotech, Nanjing, China) on an ABI-7500 Real-Time PCR System (Applied Biosystems, Beverly, MA, USA), and the relative gene expression was calculated using the standard ΔΔCt method. The specific primers used to quantify *BRE*, *BRE-AS*, *BCL2*, *BAX*, and *GAPDH* are listed in Table S3.

RACE

To determine the transcriptional initiation and termination sites in *BRE-AS*, 5′-RACE and 3′-RACE assays were performed using a SMARTer RACE cDNA Amplification Kit (TaKaRa, Dalian, China). The gene-specific primers used in these assays were 5′-TGG GGT

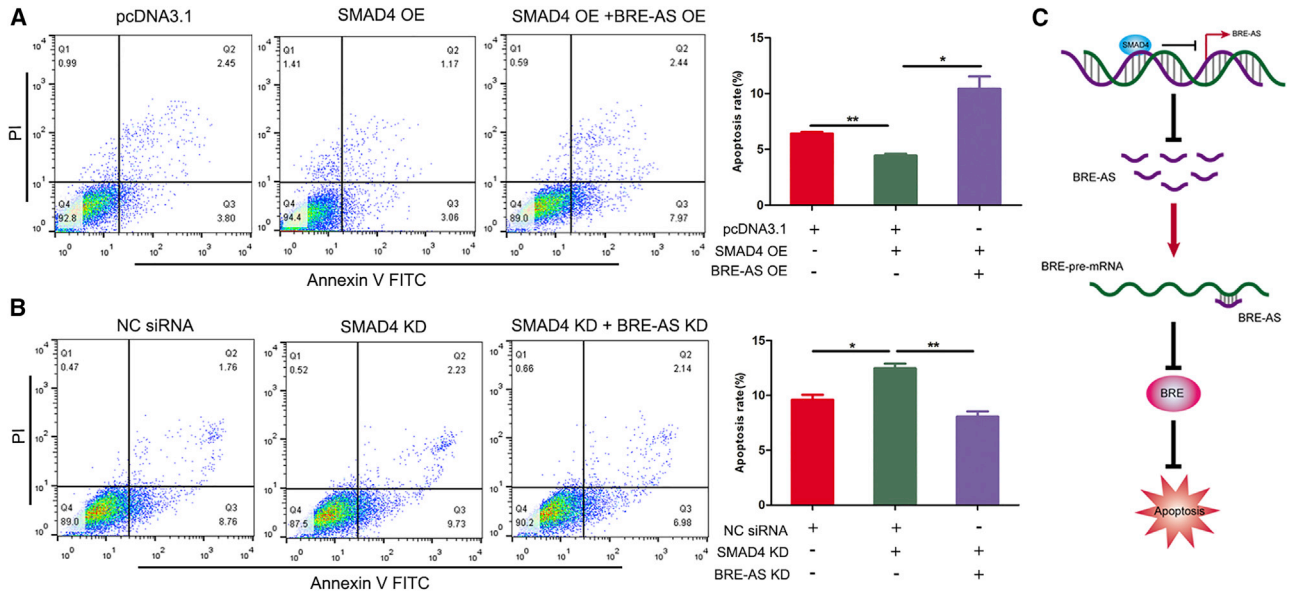

Figure 8. BRE-AS mediates SMAD4 inhibition of GC apoptosis

(A and B) GCs were co-transfected with pcDNA3.1-BRE-AS and pcDNA3.1-SMAD4 (A) or BRE-AS-siRNA and SMAD4-siRNA (B), and apoptosis rate was analyzed by FACS. (C) A model of SMAD4/*BRE-AS*/BRE pathway regulating GC apoptosis. Each group has at least 3 replicates. Each group is represented by mean ± SEM; *$p < 0.05$, **$p < 0.01$.

CTT GGG TCC ACC TGA GGT C-3′ for the 5′-RACE assay and 5′-CGG CAG AGC CAG CCA GGA TTC TGA C-3′ for the 3′-RACE assay.

Cell culture and transfection

GCs were isolated from 3- to 5-mm healthy follicles, grown in 12- or 6-well plates, and maintained in Dulbecco's modified Eagle's medium/F-12 (Gibco, Carlsbad, CA, USA) supplemented with 15% fetal bovine serum (FBS, Gibco, Carlsbad, CA, USA), 100 U/mL penicillin, and 100 μg/mL streptomycin (Gibco, Carlsbad, CA, USA). After being cultured at 37°C and 5% CO_2 for 36 h, the GCs were washed twice with PBS and prepared for transfection. KGN cell lines were obtained from Procell (Procell, Wuhan, China), maintained in Roswell Park Memorial Institute 1640 medium supplemented with 10% FBS (Gibco, Carlsbad, CA, USA), penicillin (100 U/mL), and streptomycin (100 mg/mL), and grown at 37°C in a humidified atmosphere containing 5% CO_2. Transfection was performed at 80% confluence using Lipofectamine 3000 Reagent (Invitrogen, Shanghai, China).

Plasmid and oligonucleotide construction

To construct the BRE and *BRE-AS* overexpression vectors, we cloned the full-length cDNA of *BRE* or *BRE-AS* into a pcDNA3.1 expression vector (GenePharma, Shanghai, China) using *NHE*I and *Xho*I enzymes; the pcDNA3.1-SMAD4 vector was constructed as previously described.[37] To identify the core promoter region of *BRE-AS*, 309-, 541-, 805-, and 1,100-bp fragments from the *BRE-AS* promoter region were cloned and inserted into the pGL3-Basic vector (Promega, Madison, WI, USA) using KpnI and *Xho*I. BRE-AS-, BRE-, and SMAD4-specific siRNAs were synthesized by GenePharma (Shanghai, China). All the relevant oligonucleotide sequences are summarized in Table S4.

Apoptosis assay

Cellular apoptosis was evaluated using an Annexin V-FITC/PI Apoptosis Detection Kit (Vazyme, Nanjing, China). Briefly, GCs were double-stained using 5 μL of annexin V and 5 μL of propidium iodide, and the number of apoptotic cells was calculated using a BD FACScan flow cytometry system (Becton Dickinson, Franklin, NJ, USA) with an excitation wavelength of 488 nm and an emission wavelength of 605 nm.

Western blotting

Western blotting was performed as previously described.[3] After being denaturated at 99°C for 10 min, total proteins were separated using 10%–12% sodium dodecyl sulfate polyacrylamide gel electrophoresis, transferred to polyvinylidene difluoride membranes (Merck Millipore), and probed with primary antibodies against BRE (diluted at 1:1,000, Abcam, Cambridge, MA, USA) or beta-tubulin (diluted at 1:2,000, Proteintech, China). After incubation with horseradish peroxidase-conjugated AffiniPure goat anti-rabbit immunoglobulin G (IgG) secondary antibodies (diluted at 1:5,000, Sangon Biotech, China), the antigen–antibody reactions were evaluated using an enhanced chemiluminescence reagent (Biosharp, Nanjing, China) and visualized using the Bio-Rad Quantity One 1-D system (Bio-Rad, Hercules, CA, USA).

Subcellular localization

GCs were incubated in 200 μL of cold cytoplasmic lysate buffer (0.15% NP-40, 10 μM Tris, and 150 μM NaCl) for 5 min, and then 500 μL of cold sucrose buffer (10 μM Tris, 150 μM NaCl, and 24% sucrose) was added. The samples were centrifuged at 10,000 × *g* for 3 min at 4°C. The supernatant containing the cytoplasmic components was collected and stored at −80°C. Further, the nuclei in the precipitate were resuspended in ddH_2O without RNase and centrifuged at 10,000 × *g* for 3 min at 4°C. The supernatant was removed, and the precipitate containing the nuclear components was retained. We isolated RNA from the cytoplasmic and nuclear components as described above and then performed qRT-PCR to evaluate *BRE-AS* expression.

RNA FISH assay

GCs were fixed in 4% formaldehyde for 20 min at 20°C and then permeabilized using PBS containing 0.39% Triton X-100 for 5 min on ice. After washing in PBS and 2× saline sodium citrate buffer, the cy3- and FAM-labeled oligonucleotide probes against *BRE-AS* (5′-CCG CAC GCA TCT GGA CTG GAC AGC ACA ACT-3′) and *BRE* pre-mRNA (5′-AGC AAC GCA AGA CCT CAG GTG GAC CCA AGA-3′) were incubated with the treated GCs and hybridized overnight at 37°C in a humidified chamber. The nuclei were counterstained with 4′,6-diamidino-2-phenylindole (DAPI), and *BRE-AS* and *BRE* pre-mRNA were detected using fluorescence microscopy at 543 nm and 647 nm wavelengths, respectively.

Ribonuclease protection assay (RPA)

RPA was used to identify any dsRNA in the total RNA isolated from GC samples treated with DNase I (Vazyme Biotech, Nanjing, China) and RNase I (Invitrogen, Shanghai, China), which removed all genomic DNA contamination and cleaved any ssRNA. We used a specific primer probe set designed against a non-overlapping and overlapping region of the transcript to detect degradation via PCR. The sequences for the primers used in these assays are described in Table S3.

Luciferase reporter assay

Luciferase activity was measured using Luciferase Assay Buffer II and Stop & GLO Substrate using a Modulus Assay System (Promega, Madison, WI, USA) according to the manufacturer's instructions. The firefly and Renilla luciferase activity were then evaluated and normalized for each sample.

ChIP assay

The ChIP assay was performed using a Pierce Agarose ChIP Kit (Thermo Scientific, Waltham, MA, USA). Briefly, a total of 2×10^6 cells were fixed in 1% formaldehyde via gentle swirling at 20°C for 10 min, and the fixing reaction was stopped by the addition of glycine solution. Nucleic acid was digested into 300–600-bp fragments using 6 U of micrococcal nuclease incubated in a water bath at 37°C for 15 min. IP samples were incubated with 2 μg of SMAD4 antibody or normal rabbit IgG overnight at 4°C on a rocking platform, and precipitated DNA fragments containing SBE motifs were detected using PCR with the specific primers listed in Table S3.

Statistical analysis

Data are presented as mean ± standard error of mean, and IBM SPSS Statistics v.20.0 (SPSS) was used for all statistical analyses. Significance of data was evaluated using Student's t test or one-way analysis of variance. *$p < 0.05$ and **$p < 0.01$ were considered to indicate statistical significance, and GraphPad Prism v.5.0 software was used to create all figures.

SUPPLEMENTAL INFORMATION

Supplemental information can be found online at https://doi.org/10.1016/j.omtn.2021.05.006.

ACKNOWLEDGMENTS

This work was supported by the Qing Lan Project of Jiangsu Province (2020) and the National Natural Science Foundation of China (no. 31772568).

AUTHOR CONTRIBUTIONS

W.Y. and Q.L. designed the research; W.Y., X.D., and M.W. performed the experiments; W.Y., Y.W., and Z.P. analyzed the data; W.Y., J.Z., and Q.L. wrote the manuscript.

DECLARATION OF INTERESTS

The authors declare no competing interests.

REFERENCES

1. Wang, P., Xue, Y., Han, Y., Lin, L., Wu, C., Xu, S., Jiang, Z., Xu, J., Liu, Q., and Cao, X. (2014). The STAT3-binding long noncoding RNA lnc-DC controls human dendritic cell differentiation. Science *344*, 310–313.

2. Ranzani, V., Rossetti, G., Panzeri, I., Arrigoni, A., Bonnal, R.J., Curti, S., Gruarin, P., Provasi, E., Sugliano, E., Marconi, M., et al. (2015). The long intergenic noncoding RNA landscape of human lymphocytes highlights the regulation of T cell differentiation by linc-MAF-4. Nat. Immunol. *16*, 318–325.

3. Du, X., Liu, L., Li, Q., Zhang, L., Pan, Z., and Li, Q. (2020). NORFA, long intergenic noncoding RNA, maintains sow fertility by inhibiting granulosa cell death. Commun. Biol. *3*, 131.

4. Daneshvar, K., Ardehali, M.B., Klein, I.A., Hsieh, F.K., Kratkiewicz, A.J., Mahpour, A., Cancelliere, S.O.L., Zhou, C., Cook, B.M., Li, W., et al. (2020). lncRNA DIGIT and BRD3 protein form phase-separated condensates to regulate endoderm differentiation. Nat. Cell Biol. *22*, 1211–1222.

5. St Laurent, G., Wahlestedt, C., and Kapranov, P. (2015). The Landscape of long noncoding RNA classification. Trends Genet. *31*, 239–251.

6. Latgé, G., Poulet, C., Bours, V., Josse, C., and Jerusalem, G. (2018). Natural antisense transcripts: molecular mechanisms and implications in breast cancers. Int. J. Mol. Sci. *19*, 123.

7. Faghihi, M.A., and Wahlestedt, C. (2009). Regulatory roles of natural antisense transcripts. Nat. Rev. Mol. Cell Biol. *10*, 637–643.

8. Hu, S., Wang, X., and Shan, G. (2016). Insertion of an Alu element in a lncRNA leads to primate-specific modulation of alternative splicing. Nat. Struct. Mol. Biol. *23*, 1011–1019.

9. d'Ydewalle, C., Ramos, D.M., Pyles, N.J., Ng, S.Y., Gorz, M., Pilato, C.M., Ling, K., Kong, L., Ward, A.J., Rubin, L.L., et al. (2017). The antisense transcript SMN-AS1 regulates SMN expression and is a novel therapeutic target for spinal muscular atrophy. Neuron *93*, 66–79.

10. Romero-Barrios, N., Legascue, M.F., Benhamed, M., Ariel, F., and Crespi, M. (2018). Splicing regulation by long noncoding RNAs. Nucleic Acids Res. *46*, 2169–2184.

11. Hu, J., Qian, Y., Peng, L., Ma, L., Qiu, T., Liu, Y., Li, X., and Chen, X. (2018). Long noncoding RNA EGFR-AS1 promotes cell proliferation by increasing EGFR mRNA stability in gastric cancer. Cell. Physiol. Biochem. *49*, 322–334.

12. Li, B., Hu, Y., Li, X., Jin, G., Chen, X., Chen, G., Chen, Y., Huang, S., Liao, W., Liao, Y., et al. (2018). Sirt1 antisense long noncoding RNA promotes cardiomyocyte proliferation by enhancing the stability of Sirt1. J. Am. Heart Assoc. *7*, e009700.

13. Goldstein, B., Agranat-Tamir, L., Light, D., Ben-Naim Zgayer, O., Fishman, A., and Lamm, A.T. (2017). A-to-I RNA editing promotes developmental stage-specific gene and lncRNA expression. Genome Res. *27*, 462–470.

14. McHugh, C.A., Chen, C.K., Chow, A., Surka, C.F., Tran, C., McDonel, P., Pandya-Jones, A., Blanco, M., Burghard, C., Moradian, A., et al. (2015). The Xist lncRNA interacts directly with SHARP to silence transcription through HDAC3. Nature *521*, 232–236.

15. Colognori, D., Sunwoo, H., Kriz, A.J., Wang, C.Y., and Lee, J.T. (2019). Xist deletional analysis reveals an interdependency between Xist RNA and polycomb complexes for spreading along the inactive X. Mol. Cell *74*, 101–117.e10.

16. Bernardes de Jesus, B., Marinho, S.P., Barros, S., Sousa-Franco, A., Alves-Vale, C., Carvalho, T., and Carmo-Fonseca, M. (2018). Silencing of the lncRNA Zeb2-NAT facilitates reprogramming of aged fibroblasts and safeguards stem cell pluripotency. Nat. Commun. *9*, 94.

17. Canzio, D., Nwakeze, C.L., Horta, A., Rajkumar, S.M., Coffey, E.L., Duffy, E.E., Duffié, R., Monahan, K., O'Keeffe, S., Simon, M.D., et al. (2019). Antisense lncRNA transcription mediates DNA demethylation to drive stochastic protocadherin alpha promoter choice. Cell *177*, 639–653.e15.

18. Xue, Z., Ye, Q., Anson, S.R., Yang, J., Xiao, G., Kowbel, D., Glass, N.L., Crosthwaite, S.K., and Liu, Y. (2014). Transcriptional interference by antisense RNA is required for circadian clock function. Nature *514*, 650–653.

19. Wang, Y., Yang, L., Chen, T., Liu, X., Guo, Y., Zhu, Q., Tong, X., Yang, W., Xu, Q., Huang, D., and Tu, K. (2019). A novel lncRNA MCM3AP-AS1 promotes the growth of hepatocellular carcinoma by targeting miR-194-5p/FOXA1 axis. Mol. Cancer *18*, 28.

20. Li, Y., Guo, D., Lu, G., Mohiuddin Chowdhury, A.T.M., Zhang, D., Ren, M., Chen, Y., Wang, R., and He, S. (2020). LncRNA SNAI3-AS1 promotes PEG10-mediated proliferation and metastasis via decoying of miR-27a-3p and miR-34a-5p in hepatocellular carcinoma. Cell Death Dis. *11*, 685.

21. Kimura, A.P., Yoneda, R., Kurihara, M., Mayama, S., and Matsubara, S. (2017). A long noncoding RNA, lncRNA-Amhr2, plays a role in Amhr2 gene activation in mouse ovarian granulosa cells. Endocrinology *158*, 4105–4121.

22. Yung, Y., Ophir, L., Yerushalmi, G.M., Baum, M., Hourvitz, A., and Maman, E. (2019). HAS2-AS1 is a novel LH/hCG target gene regulating HAS2 expression and enhancing cumulus cells migration. J. Ovarian Res. *12*, 21.

23. Zhang, C., Wu, W., Ye, X., Ma, R., Luo, J., Zhu, H., and Chang, X. (2019). Aberrant expression of CHL1 gene and long non-coding RNA CHL1-AS1, CHL1-AS2 in ovarian endometriosis. Eur. J. Obstet. Gynecol. Reprod. Biol. *236*, 177–182.

24. Zhu, H.L., Chen, Y.Q., and Zhang, Z.F. (2020). Downregulation of lncRNA ZFAS1 and upregulation of microRNA-129 repress endocrine disturbance, increase proliferation and inhibit apoptosis of ovarian granulosa cells in polycystic ovarian syndrome by downregulating HMGB1. Genomics *112*, 3597–3608.

25. Dewailly, D., Robin, G., Peigne, M., Decanter, C., Pigny, P., and Catteau-Jonard, S. (2016). Interactions between androgens, FSH, anti-Müllerian hormone and estradiol during folliculogenesis in the human normal and polycystic ovary. Hum. Reprod. Update *22*, 709–724.

26. Zhang, J., Xu, Y., Liu, H., and Pan, Z. (2019). MicroRNAs in ovarian follicular atresia and granulosa cell apoptosis. Reprod. Biol. Endocrinol. *17*, 9.

27. Zhou, J., Peng, X., and Mei, S. (2019). Autophagy in ovarian follicular development and atresia. Int. J. Biol. Sci. *15*, 726–737.

28. Matsuda, F., Inoue, N., Manabe, N., and Ohkura, S. (2012). Follicular growth and atresia in mammalian ovaries: regulation by survival and death of granulosa cells. J. Reprod. Dev. *58*, 44–50.

29. Yeung, C.K., Wang, G., Yao, Y., Liang, J., Tenny Chung, C.Y., Chuai, M., Lee, K.K., and Yang, X. (2017). BRE modulates granulosa cell death to affect ovarian follicle development and atresia in the mouse. Cell Death Dis. *8*, e2697.

30. Tiwari, M., Prasad, S., Tripathi, A., Pandey, A.N., Ali, I., Singh, A.K., Shrivastav, T.G., and Chaube, S.K. (2015). Apoptosis in mammalian oocytes: a review. Apoptosis *20*, 1019–1025.

31. Chu, Y.L., Xu, Y.R., Yang, W.X., and Sun, Y. (2018). The role of FSH and TGF-β superfamily in follicle atresia. Aging (Albany NY) *10*, 305–321.

32. Liu, J., Li, X., Yao, Y., Li, Q., Pan, Z., and Li, Q. (2018). miR-1275 controls granulosa cell apoptosis and estradiol synthesis by impairing LRH-1/CYP19A1 axis. Biochim. Biophys. Acta. Gene Regul. Mech. *1861*, 246–257.

33. Li, Q., Du, X., Wang, L., Shi, K., and Li, Q. (2021). TGF-β1 controls porcine granulosa cell states: A miRNA-mRNA network view. Theriogenology *160*, 50–60.

34. Du, X., Liu, L., Wu, W., Li, P., Pan, Z., Zhang, L., Liu, J., and Li, Q. (2020). SMARCA2 is regulated by *NORFA*-miR-29c, a novel pathway that controls granulosa cell apoptosis and is related to female fertility. J. Cell Sci. *133*, jcs249961.

35. Guo, T., Zhang, J., Yao, W., Du, X., Li, Q., Huang, L., Ma, M., Li, Q., Liu, H., and Pan, Z. (2019). CircINHA resists granulosa cell apoptosis by upregulating CTGF as a ceRNA of miR-10a-5p in pig ovarian follicles. Biochim. Biophys. Acta. Gene Regul. Mech. *1862*, 194420.

36. Salameh, A., Lee, A.K., Cardó-Vila, M., Nunes, D.N., Efstathiou, E., Staquicini, F.I., Dobroff, A.S., Marchiò, S., Navone, N.M., Hosoya, H., et al. (2015). PRUNE2 is a human prostate cancer suppressor regulated by the intronic long noncoding RNA PCA3. Proc. Natl. Acad. Sci. USA *112*, 8403–8408.

37. Zhang, L., Du, X., Wei, S., Li, D., and Li, Q. (2016). A comprehensive transcriptomic view on the role of SMAD4 gene by RNAi-mediated knockdown in porcine follicular granulosa cells. Reproduction *152*, 81–89.

38. Liu, J., Du, X., Zhou, J., Pan, Z., Liu, H., and Li, Q. (2014). MicroRNA-26b functions as a proapoptotic factor in porcine follicular Granulosa cells by targeting Sma-and Mad-related protein 4. Biol. Reprod. *91*, 146.

39. Han, Y., Wang, S., Wang, Y., and Zeng, S. (2019). IGF-1 inhibits apoptosis of porcine primary granulosa cell by targeting degradation of BimEL. Int. J. Mol. Sci. *20*, 5356.

40. Zhang, J., Zhang, J., Gao, B., Xu, Y., Liu, H., and Pan, Z. (2019). Detection of the effects and potential interactions of FSH, VEGFA, and 2-methoxyestradiol in follicular angiogenesis, growth, and atresia in mouse ovaries. Mol. Reprod. Dev. *86*, 566–575.

41. Shen, M., Cao, Y., Jiang, Y., Wei, Y., and Liu, H. (2018). Melatonin protects mouse granulosa cells against oxidative damage by inhibiting FOXO1-mediated autophagy: Implication of an antioxidation-independent mechanism. Redox Biol. *18*, 138–157.

42. Lin, F., Fu, Y.H., Han, J., Shen, M., Du, C.W., Li, R., Ma, X.S., and Liu, H.L. (2014). Changes in the expression of Fox O1 and death ligand genes during follicular atresia in porcine ovary. Genet. Mol. Res. *13*, 6638–6645.

43. Du, X., Li, Q., Yang, L., Liu, L., Cao, Q., and Li, Q. (2020). SMAD4 activates Wnt signaling pathway to inhibit granulosa cell apoptosis. Cell Death Dis. *11*, 373.

44. Hu, X., Kim, J.A., Castillo, A., Huang, M., Liu, J., and Wang, B. (2011). NBA1/MERIT40 and BRE interaction is required for the integrity of two distinct deubiquitinating enzyme BRCC36-containing complexes. J. Biol. Chem. *286*, 11734–11745.

45. Biswas, K., Philip, S., Yadav, A., Martin, B.K., Burkett, S., Singh, V., Babbar, A., North, S.L., Chang, S., and Sharan, S.K. (2018). BRE/BRCC45 regulates CDC25A stability by recruiting USP7 in response to DNA damage. Nat. Commun. *9*, 537.

46. Li, L., Yoo, H., Becker, F.F., Ali-Osman, F., and Chan, J.Y. (1995). Identification of a brain- and reproductive-organs-specific gene responsive to DNA damage and retinoic acid. Biochem. Biophys. Res. Commun. *206*, 764–774.

47. Chan, B.C., Ching, A.K., To, K.F., Leung, J.C., Chen, S., Li, Q., Lai, P.B., Tang, N.L., Shaw, P.C., Chan, J.Y., et al. (2008). BRE is an antiapoptotic protein in vivo and overexpressed in human hepatocellular carcinoma. Oncogene *27*, 1208–1217.

48. Li, Y., Qi, K., Zu, L., Wang, M., Wang, Y., and Zhou, Q. (2016). Anti-apoptotic brain and reproductive organ-expressed proteins enhance cisplatin resistance in lung cancer cells via the protein kinase B signaling pathway. Thorac. Cancer *7*, 190–198.

49. Jin, F., Zhu, Y., Chen, J., Wang, R., Wang, Y., Wu, Y., Zhou, P., Song, X., Ren, Z., and Dong, J. (2020). BRE promotes esophageal squamous cell carcinoma growth by activating AKT signaling. Front. Oncol. *10*, 1407.

50. Merkle, T., Merz, S., Reautschnig, P., Blaha, A., Li, Q., Vogel, P., Wettengel, J., Li, J.B., and Stafforst, T. (2019). Precise RNA editing by recruiting endogenous ADARs with antisense oligonucleotides. Nat. Biotechnol. *37*, 133–138.

51. Zhao, X., Li, J., Lian, B., Gu, H., Li, Y., and Qi, Y. (2018). Global identification of Arabidopsis lncRNAs reveals the regulation of MAF4 by a natural antisense RNA. Nat. Commun. *9*, 5056.

52. Wanowska, E., Kubiak, M.R., Rosikiewicz, W., Makalowska, I., and Szcześniak, M.W. (2018). Natural antisense transcripts in diseases: from modes of action to targeted therapies. Wiley Interdiscip. Rev. RNA *9*, e1461.

53. Postepska-Igielska, A., Giwojna, A., Gasri-Plotnitsky, L., Schmitt, N., Dold, A., Ginsberg, D., and Grummt, I. (2015). LncRNA Khps1 regulates expression of the proto-oncogene SPHK1 via triplex-mediated changes in chromatin structure. Mol. Cell *60*, 626–636.

54. Su, W., Xu, M., Chen, X., Chen, N., Gong, J., Nie, L., Li, L., Li, X., Zhang, M., and Zhou, Q. (2017). Long noncoding RNA ZEB1-AS1 epigenetically regulates the expressions of ZEB1 and downstream molecules in prostate cancer. Mol. Cancer *16*, 142.

55. Villamizar, O., Chambers, C.B., Riberdy, J.M., Persons, D.A., and Wilber, A. (2016). Long noncoding RNA Saf and splicing factor 45 increase soluble Fas and resistance to apoptosis. Oncotarget *7*, 13810–13826.

56. Deng, S.J., Chen, H.Y., Zeng, Z., Deng, S., Zhu, S., Ye, Z., He, C., Liu, M.L., Huang, K., Zhong, J.X., et al. (2019). Nutrient stress-dysregulated antisense lncRNA GLS-AS impairs GLS-mediated metabolism and represses pancreatic cancer progression. Cancer Res. *79*, 1398–1412.

57. Du, X., Pan, Z., Li, Q., Liu, H., and Li, Q. (2018). SMAD4 feedback regulates the canonical TGF-β signaling pathway to control granulosa cell apoptosis. Cell Death Dis. *9*, 151.

58. Du, X., Zhang, L., Li, X., Pan, Z., Liu, H., and Li, Q. (2016). TGF-β signaling controls FSHR signaling-reduced ovarian granulosa cell apoptosis through the SMAD4/miR-143 axis. Cell Death Dis. *7*, e2476.

59. Yang, L., Du, X., Liu, L., Cao, Q., Pan, Z., and Li, Q. (2019). miR-1306 mediates the feedback regulation of the TGF-beta/SMAD signaling pathway in granulosa cells. Cells *8*, 298.

60. Lang, C., Dai, Y., Wu, Z., Yang, Q., He, S., Zhang, X., Guo, W., Lai, Y., Du, H., Wang, H., et al. (2020). SMAD3/SP1 complex-mediated constitutive active loop between lncRNA PCAT7 and TGF-β signaling promotes prostate cancer bone metastasis. Mol. Oncol. *14*, 808–828.

61. Zhang, Y.Y., Tang, P.M., Tang, P.C., Xiao, J., Huang, X.R., Yu, C., Ma, R.C.W., and Lan, H.Y. (2019). LRNA9884, a novel Smad3-dependent long noncoding RNA, promotes diabetic kidney injury in db/db mice via enhancing MCP-1-dependent renal inflammation. Diabetes *68*, 1485–1498.

62. Zhang, C., Hao, Y., Wang, Y., Xu, J., Teng, Y., and Yang, X. (2018). TGF-beta/SMAD4-regulated lncRNA-LINP1 inhibits epithelial-mesenchymal transition in lung cancer. Int. J. Biol. Sci. *14*, 1715–1723.

63. Zhuang, J., Shen, L., Yang, L., Huang, X., Lu, Q., Cui, Y., Zheng, X., Zhao, X., Zhang, D., Huang, R., et al. (2017). TGFbeta1 promotes gemcitabine resistance through regulating the lncRNA-LET/NF90/miR-145 signaling axis in bladder cancer. Theranostics *7*, 3053–3067.

64. Luo, S., Lu, J.Y., Liu, L., Yin, Y., Chen, C., Han, X., Wu, B., Xu, R., Liu, W., Yan, P., et al. (2016). Divergent lncRNAs regulate gene expression and lineage differentiation in pluripotent cells. Cell Stem Cell *18*, 637–652.

65. Wang, L., Park, H.J., Dasari, S., Wang, S., Kocher, J.P., and Li, W. (2013). CPAT: Coding-Potential Assessment Tool using analignment-free logistic regression model. Nucleic Acids Res. *41*, e74.